Journal of Power Sources 196 (2011) 8955–8966

Contents lists available at ScienceDirect

Journal of Power Sources

journal homepage: www.elsevier.com/locate/jpowsour

Investigation of gas diffusion layer compression by electrochemical impedance spectroscopy on running polymer electrolyte membrane fuel cells

Giovanni Dotelli[a,*], Luca Omati[a], Paola Gallo Stampino[a], Paolo Grassini[b], Davide Brivio[b]

[a] Politecnico di Milano – Dipartimento di Chimica Materiali e Ingegneria Chimica "G. Natta", Piazza Leonardo da Vinci 32, 20133 Milano, Italy
[b] SAATI srl, via Quasimodo, Legnano, 20025 Milano, Italy

ARTICLE INFO

Article history:
Received 31 October 2010
Received in revised form 8 January 2011
Accepted 12 January 2011
Available online 28 January 2011

Keywords:
Gas diffusion layer
Microporous layer
Electrochemical impedance spectroscopy
Compression
PEM-FC

ABSTRACT

Two gas diffusion layers based on the same carbon cloth substrate, produced by an Italian Company (SAATI), and coated with microporous layers of different hydrophobicities, were assembled in a polymer electrolyte membrane fuel cell and its performances assessed. For comparison the cell mounting the carbon cloth without microporous layer was also tested. The membrane electrode assembly was made of Nafion® 212 with Pt load 0.3/0.6 mg cm^{-2} (anode/cathode). The cell testing was run at 60 °C and 80 °C with fully humidified air (100%RH) and 80%RH hydrogen feedings. The assembly of gas diffusion layers and membrane with electrodes was compressed to 30% and 50% of its initial thickness. For each configuration polarization and power curves were recorded; in order to evaluate the role of different GDLs, AC impedance spectroscopy of the running cell was also performed.

The higher compression ratio caused the worsening of cell performances, partially mitigated when the operating temperature was raised to 80 °C. The presence of the microporous layer onto the carbon cloth resulted extremely beneficial for the operations especially at high current density; moreover, it sensibly reduces the high frequency resistance of the overall assembly.

1. Introduction

Polymer electrolyte membrane (PEM) fuel cells (FCs) have been recognized as good candidates to substitute more traditional power sources in portable as well as mobile applications [1].

The operation of a PEMFC is strictly connected to the flow of reactant gases coming from outside and that have to reach the catalyst layers (CLs) coated onto the membrane passing through macro- and possibly micro-porous media [2]; however, in order to guarantee a high cell efficiency the gases are normally fed at a high relative humidity (RH) degree so that the polymeric membrane can stay fully humidified and its ionic conductivity be at its maximum. In addition to humidified gas streams the electrochemical reaction produces water whose proper management is a vital key point in FC operation [3–5].

In the years gas diffusion layer (GDL) has revealed to be a key component of PEMFCs; it plays a fundamental role in removing reaction products, i.e. water and unreacted gases, from the electrodes, but it also helps distribute homogenously the reactant gases onto the CLs as well as it is the path for electrons to and from the catalyst layer and the bipolar plate [5]. In view of this role, GDL materials have to be hydrophobic, porous and electrically conductive. Accordingly, GDLs are usually made of carbon cloth or paper, treated with different hydrophobic agents [6], and usually coated with a micro-porous layer (MPL). Recently, it has been demonstrated that the MPL reduces the number of injection sites for liquid water from the catalyst layer to the gas diffusion layer, which in turn reduces the overall saturation [7–10]. As a consequence adding the MPL to the cell sandwich leads to less water in the GDL substrate [11], cloth or paper does not matter, enhances gas transport because the risk of macropores flooding is diminished and prevents the membrane from excessive drying. However, to prevent gas leakages stacks must be compressed so GDL compression is inevitable. Of course, compression reduces porosity and pore sizes of the GDL and affects permeability, effective diffusivity and contact resistance [12–16], which in turn have an effect on the FC performances.

In the present work two gas diffusion layers based on the same carbon cloth substrate, produced by an Italian Company (SAATI), and coated with microporous layers of different hydrophobicities, were tested; for the sake of comparison the carbon cloth without microporous layer was also tested. The membrane electrode assembly was made of Nafion® 212 with Pt load 0.3/0.6 mg cm^{-2} (anode/cathode). The cell testing was run at 60 °C and 80 °C with fully humidified air (100%RH) and 80%RH hydrogen feedings. The assembly of gas diffusion layers and membrane with electrodes was compressed to 30% and 50% of its initial thickness. For each configuration *I–V* electrochemical characterization was performed to assess cell performances. AC impedance spectroscopy of the run-

* Corresponding author. Tel.: +39 02 23993232; fax: +39 02 70638173.
E-mail address: giovanni.dotelli@polimi.it (G. Dotelli).

0378-7753/$ – see front matter © 2011 Elsevier B.V. All rights reserved.
doi:10.1016/j.jpowsour.2011.01.078

Table 1
Textile properties of gas diffusion layer P10. Data are supplied by the producer.

Density (kg m^{-3})	302
Warp (threads cm^{-1})	25
Weft (threads cm^{-1})	23
Thickness @ 200 kPa (mm)[a] ASTM D646-96	325
Weight (g m^{-2})	125
Trough plane air permeability @ 100 Pa (cm s^{-1})[b] ASTM D737-96	102
In plane air permeability @ 100 Pa (mm s^{-1})	2.73
Water permeability (Pa)	11.3

[a] Two point measurement, circular (5 cm^2) gold-plated contacts.
[b] Test surface: 20 cm^2.

ning cell was carried out as well, this technique being able to split up losses into their components [17–22].

2. Experimental

2.1. Materials

The GDL used throughout this work was a carbon cloths (Table 1) produced by an Italian company (SAATI SpA, Table 1), and treated with PTFE (10 wt%) to increase its hydrophobicity. These substrates were coated with two MPLs, one with a high (40%) and low (12%) content of PTFE to make them more hydrophobic. Carbon powder, Vulcan XC72R (CB in the following), 60 wt% PTFE emulsion, Triton X100 surfactant (T in the following) and deionized water (W in the following) were used to prepare the inks for the MPL. The slurries were deposited onto the substrates via doctor-blade technique using lab-scale commercial equipment K CONTROL COATER. A linear velocity of 0.0625 m s^{-1} and a 40 μm gap were selected, corresponding to a shear rate of about 170 s^{-1}. The coated samples were calcined up to 370 °C for 30 min [23].

In the following the carbon cloth without MPL will be labelled P10 and the other two GDLs coated with the micro-porous layer will be referred to as MPL12 and MPL40, remarking the content of the hydrophobic agent.

2.2. Electronic microscopy

A Cambridge Stereoscan 360 scanning electron microscope (SEM) was used for the morphological analysis of the samples. SEM analyses were carried out both onto the surfaces and the fracture surfaces of the samples, that were gold coated to prevent charging effects.

2.3. Electrochemical I–V cell performance

Electrochemical performances of the GDLs were tested in a single cell (Fuel Cell Technologies). The bipolar plates (BP) have a single serpentine at the anode and a triple parallel serpentine at the cathode side. The GDLs were placed at the anode and cathode side clamping the screw of the cell at a torque of about 10 Nm. The compression of GDLs was fixed at 30% and 50% of the original thickness and kept constant with the use of uncompressible glass fiber gaskets. The compression ratio (CR) of the GDL is defined as the ratio of the decrease in thickness to its original one, i.e. $(h - h_0)/h_0$%. The MEA was assembled using a Nafion® 212 membrane with a thickness of 50 μm and an active area of 25 cm^2; the catalyst layer was coated directly onto the membrane with a platinum loading of 0.3 mg cm^{-2} at the anode (A) and of 0.6 mg cm^{-2} at the cathode (C). Pure hydrogen and air were fed at the anode and cathode, respectively. The flow rates were 0.2 Nl min^{-1} of hydrogen and 1.0 Nl min^{-1} of air, corresponding to a stoichiometric ratio $S = 1.2/2.0$ A/C @ 1 A cm^{-2}, and were controlled and detected by a calibrated flow meter. The degree of humidity and the gas temperature were controlled by saturators and temperature controllers: the temperature of the cell was kept at 60 °C and 80 °C, the relative humidity of reactants was kept constant both for anode and cathode. In particular, at the anode it was set at 80%RH, while at the cathode at 100%RH. An electronic load (RBL488-50-150-800) was connected to the cell, which measures and controls the voltage, the current and the generated electric power. Polarization curves were recorded under galvanostatic conditions in the current density range from OCV to 0.87 A cm^{-2}, with steps of 0.085 A cm^{-2}, and at each step the resulting potential was recorded (galvanostatic mode, 420 s per step, 1pt per s recorded). Potential values plotted in the steady-state polarization curves result from the averaging of the last 300 pts recorded at each step in order to minimize experimental artefacts due to transient phenomena.

2.4. Electrochemical impedance spectroscopy

Electrochemical impedance spectroscopy (EIS) of the running FC was performed using a Frequency Response Analyzer (F.R.A.) Solartron 1260, directly connected to the electronic load (RBL488-50-150-800). This technique is able to distinguish between the influence of different electrochemical processes, especially when the system involves multiple-step reactions, parallel reactions or additional processes and to highlight the most influencing factors on cell performances [17–20]. EIS was performed in galvanostatic mode using an AC signal of amplitude 200 mA. Impedance spectra were collected by sweeping frequencies over the range 0.5 Hz to 1 kHz, acquiring 10 pts per decade. The EIS spectra were recorded at OCV and from low to high current density (i.e. 0.17, 0.34, 0.52, 0.7 and 0.87 A cm^{-2}). Five full spectra per each current density value were acquired and the impedance spectrum finally used in the discussion was the result of an averaging procedure.

The typical spectrum of a running FC is composed of one or two arcs, whose origin can be traced back to two well distinguished physical phenomena: activation polarization and mass transfer limitations. The activation polarization happens at both electrodes, but the oxygen reduction reaction (ORR) requires higher overpotentials and it is slower than hydrogen oxidation. The mass transfer limitation takes place when the reactants concentration decreases near the catalyst layer. This phenomenon more likely occurs when the cell is operating in the high current density region because higher amounts of water are produced at the cathode, increasing the risk of flooding. The reactant shortage on the active layer is magnified by using a low stoichiometric ratio.

The experimental spectra were modelled with equivalent circuits using the Zview® software (Scribner Associates). The equivalent circuit used [22] is made of a resistance (Rs) in series with two parallel capacitance/resistance circuits, (Rp/Cdl) and (Rd/Cd). Rs represents the ohmic losses, while the first circuit (Rp/Cdl) models the activation polarization (i.e. charge transfer resistance) and the second one (Rd/Cd) the losses related to the flooding phenomena (i.e. mass transfer resistance). Constant phase elements (CPE) were used instead of pure capacitances, to account for the capacitive losses that generally occur in porous electrodes [24]; in fact, the phase of CPE parameters did not dramatically deviate from unity (0.85–1.00).

3. Results and discussion

3.1. Surface morphology and thickness

Fig. 1 shows the surface morphology of the three GDLs (a, c, and e). P10 is a typical carbon cloth whose main physical properties are reported in Table 1 and which was made more hydrophobic with the usual treatment by PTFE (10 wt%). In samples MPL12 and

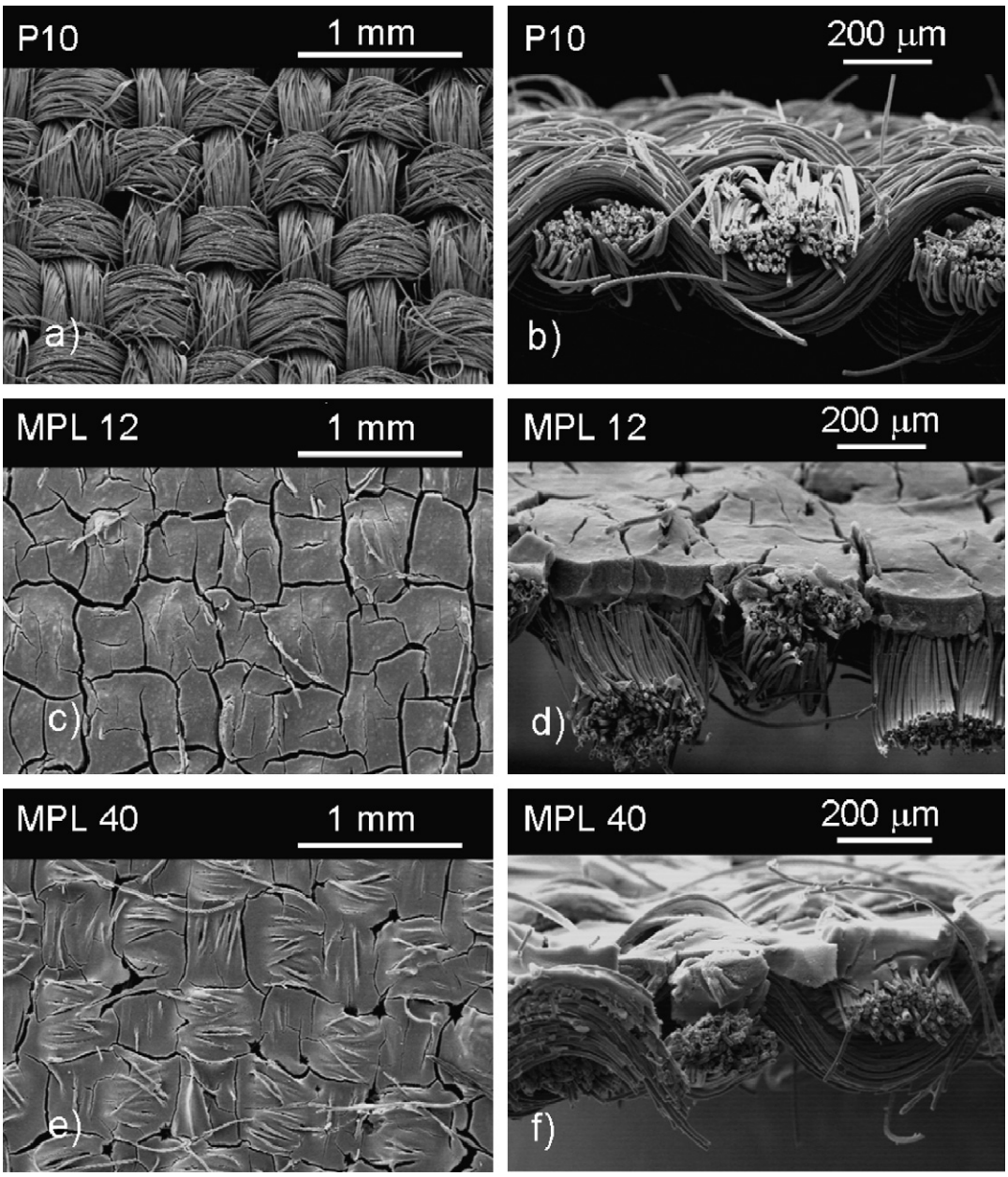

Fig. 1. SEM images of GDLs: surface (a, c, and d) and section (b, d, and f) micrographs of P10, MPL12, and MPL40, respectively.

MPL40 the same carbon cloth was coated with a MPL. The underlying warp–weft texture is unrecognizable in MPL12, while it is somewhat visible in MPL40; accordingly, the MPL thickness is more uniform in MPL12 than in MPL40 (Fig. 1d and f). On the basis of a rough estimate made on SEM micrographs of GDL sections the MPL thickness is about 50 μm in MPL12 and 20–30 μm in MPL40.

In plane electrical resistivity of the MPL12 (Table 2) is somewhat lower than that of the two other GDLs, confirming what observed in SEM images that the surface is smoother than that of the other two samples. A certain effect of the hydrophobic agent could be accounted for when MPL12 and MPL40 are compared.

On the surface there were some cracks, probably due to the calcination; but this is quite usual, as they are also found on other commercial products [25].

Previous contact angle measurements [23] confirmed the increasing hydrophobicity of the surface passing from P10 to MPL12 and MPL40 (Table 2).

Table 2
Physical properties of the three gas diffusion layers [23]; thicknesses are based on SEM micrographs.

Sample	Contact Angle (°)	In plane electrical resistivity (Ω)	Thickness (μm)
P10	133	0.86	~400
MPL12	140	0.74	~450
MPL40	143	0.83	~420–430

3.2. Cell performances

Performances of the cell mounting the three different GDLs are shown in Fig. 2, i.e. polarization and power density curves.

3.2.1. Effect of temperature

The cell was operated at 60 and 80 °C and, as expected, its performances always improved upon increasing the temperature. Indeed, the temperature enhances the ionic conductivity of PFSA mem-

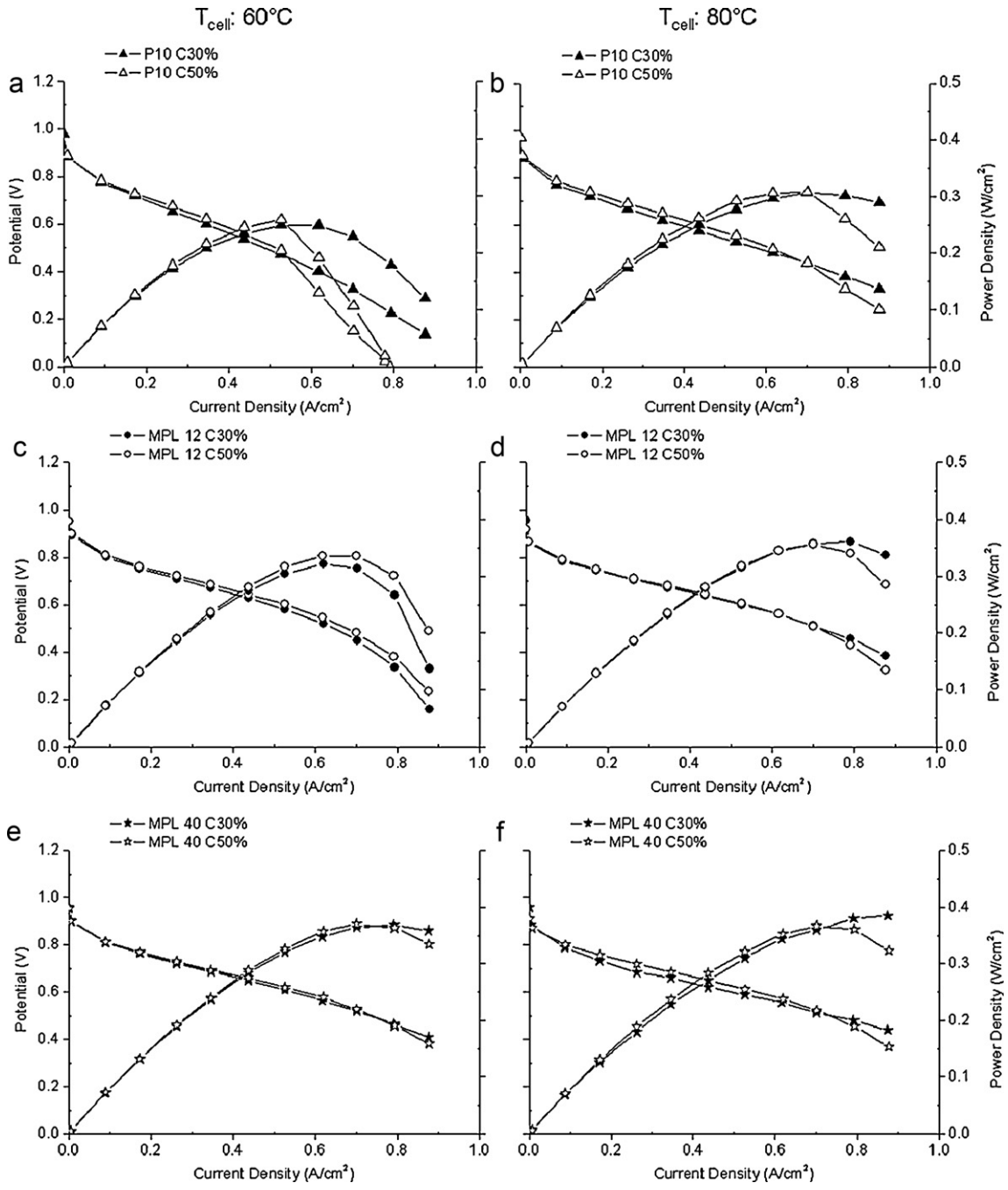

Fig. 2. Polarization and power density curves of the cell assembled with P10, MPL12, and MPL40 GDLs at two levels of compression (i.e. 30 and 50%). The cell operates at 60 °C (a, c, and e) and at 80 °C (b, d, and f).

branes as far as their humidity content does not fall off; evidently, this was not the case here and, whichever the GDL used, the water content in the membrane was preserved. The only remark could be that, passing from 60 to 80 °C, the least improvement was registered with the MPL40 and this is not surprising because it is the GDL which has the most hydrophobic MPL.

3.2.2. Effect of compression ratio

The compression ratio (CR) affects only slightly the cell performances in the low-medium current density (CD) range; on the contrary, high CR worsens the cell performances, whatever the operating temperature, at high CD, just when the water produced by the reaction is at its maximum. Clearly, the compression entails a worst water management, which is, however, somewhat mitigated by the temperature increase. Similar findings were experimentally registered by Ge et al. [15] and confirmed also by simulation [13]. For instance, when the cell operates at 60 °C the use of P10 GDL (Fig. 2a) at CR = 50% causes a dramatic collapse at high CD, which is shifted to higher CD upon increasing the temperature (Fig. 2b). In any case, when the CD exceeds 0.8 A cm^{-2} the worsening is clear even at 80 °C.

3.2.3. Influence of MPL and hydrophobic agent

The MPL coated onto the carbon cloth clearly improves the cell performances. This is very evident by comparing the results of P10 vs. MPL12 or MPL40 in Fig. 2. The maximum power generated is in the order of 0.35 W cm^{-2} or more whenever there is the MPL (Fig. 2c–f), while it reaches at most 0.30 W cm^{-2} with P10. Further-

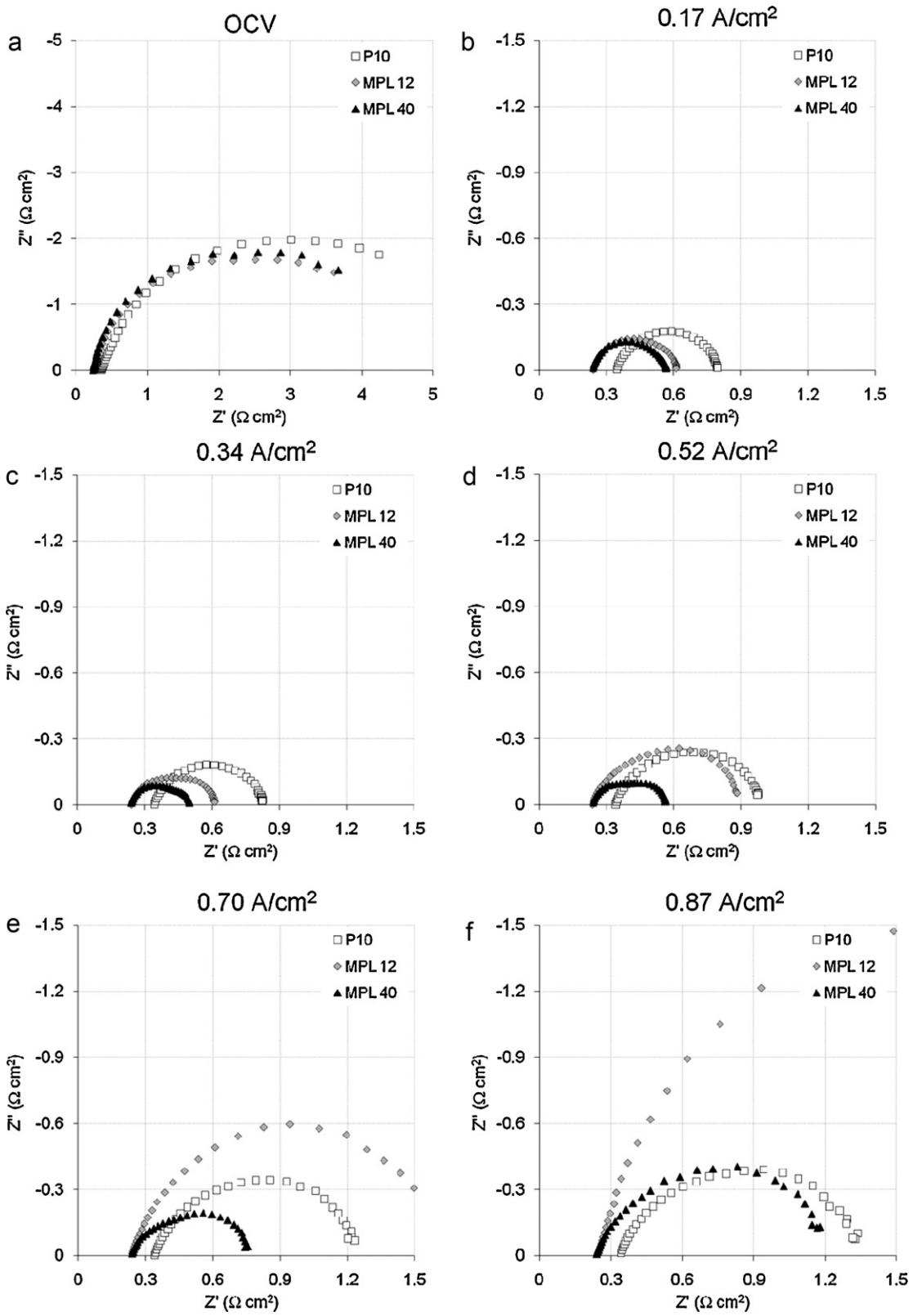

Fig. 3. Impedance spectra of the unit cell operating at 60 °C with a CR of 30% at increasing CD: (a) OCV, (b) 0.17 A cm^{-2}, (c) 0.34 A cm^{-2}, (d) 0.52 A cm^{-2}, (e) 0.70 A cm^{-2}, and (f) 0.87 A cm^{-2}.

more, the MPL mitigates the adverse effect of the high CR (50%) at high CD. The influence of the hydrophobic agent content in the MPL has a minor influence on the cell performances, and becomes more evident only at high CD. Anyway, MPL40 seems to impart better performances than MPL12. The optimal behaviour of MPL40 at high CD is not surprising because its hydrophobicity, as demonstrated by the contact angle (Table 2), helps the water management particularly when more water is generated.

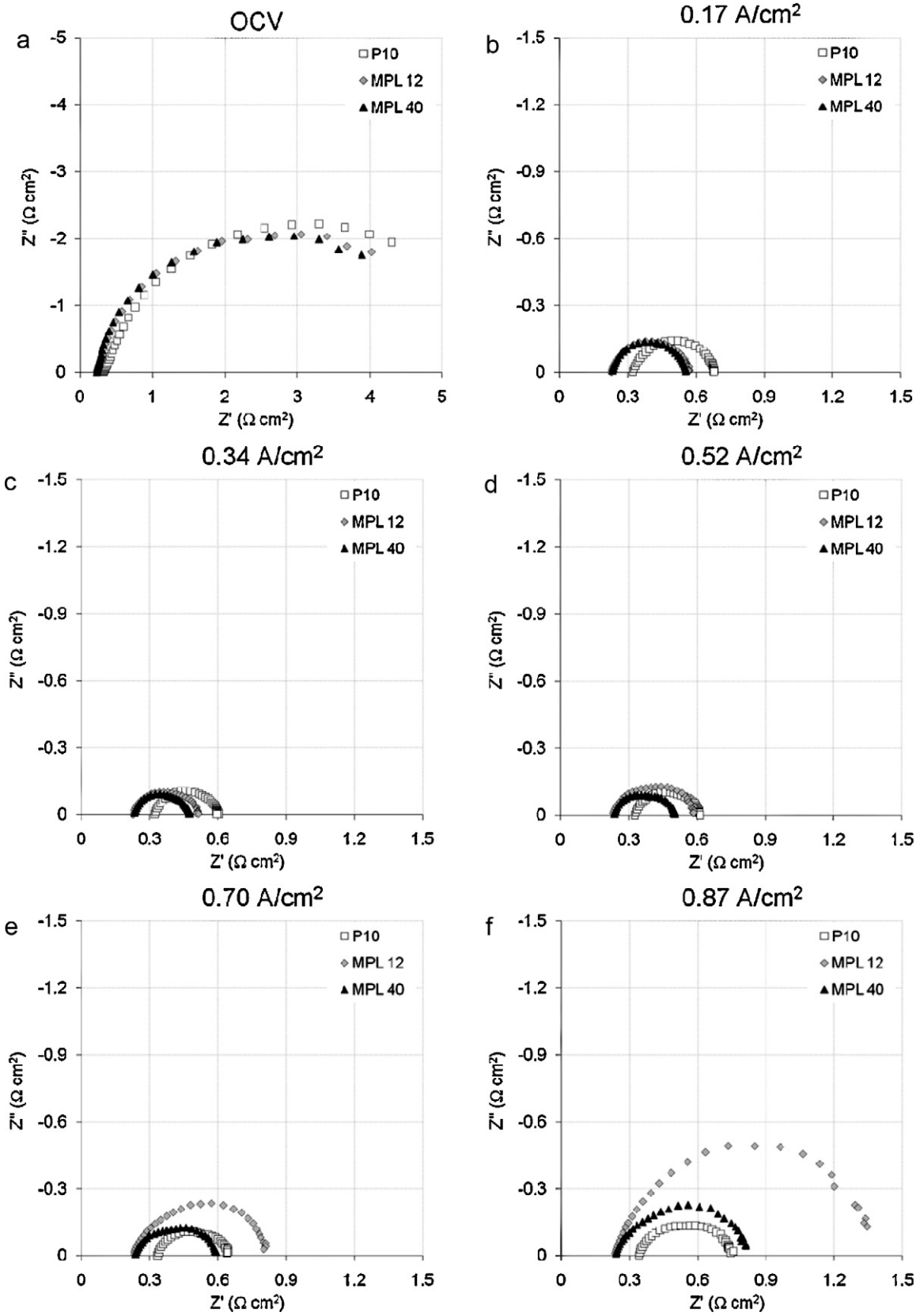

Fig. 4. Impedance spectra of the unit cell operating at 80 °C with a CR of 30% at increasing CD: (a) OCV, (b) 0.17 A cm^{-2}, (c) 0.34 A cm^{-2}, (d) 0.52 A cm^{-2}, (e) 0.70 A cm^{-2}, and (f) 0.87 A cm^{-2}.

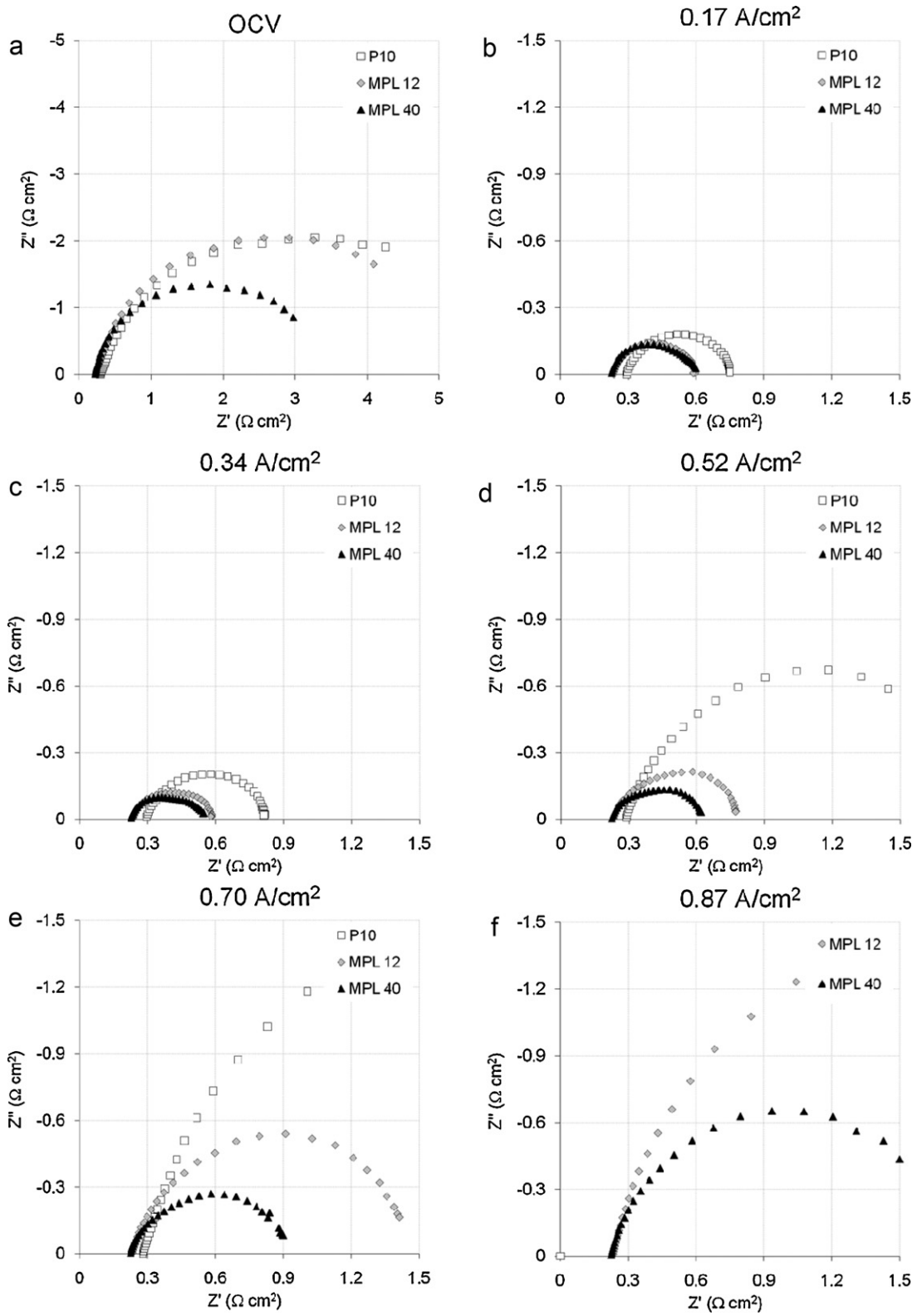

Fig. 5. Impedance spectra of the unit cell operating at 60 °C with a CR of 50% at increasing CD: (a) OCV, (b) 0.17 A cm^{-2}, (c) 0.34 A cm^{-2}, (d) 0.52 A cm^{-2}, (e) 0.70 A cm^{-2}, and (f) 0.87 A cm^{-2}.

3.3. Impedance spectroscopy

In Figs. 3 and 4 impedance spectra of the running cell with the three different assemblies (P10, MPL12, MPL40) at a CR of 30% are reported at increasing CD. All the spectra are shifted to the right because of the high frequency resistance or ohmic resistance, which is almost invariant for any specific assembly upon varying the CD, but with a marked difference between the GDLs without (P10) and with the MPL (MPL12 and MPL40).

Starting from 0.34 A cm^{-2} two overlapped semicircles can be clearly distinguished in all impedance spectra. On the contrary, at open circuit voltage (OCV) and 0.17 A cm^{-2} the spectra resemble

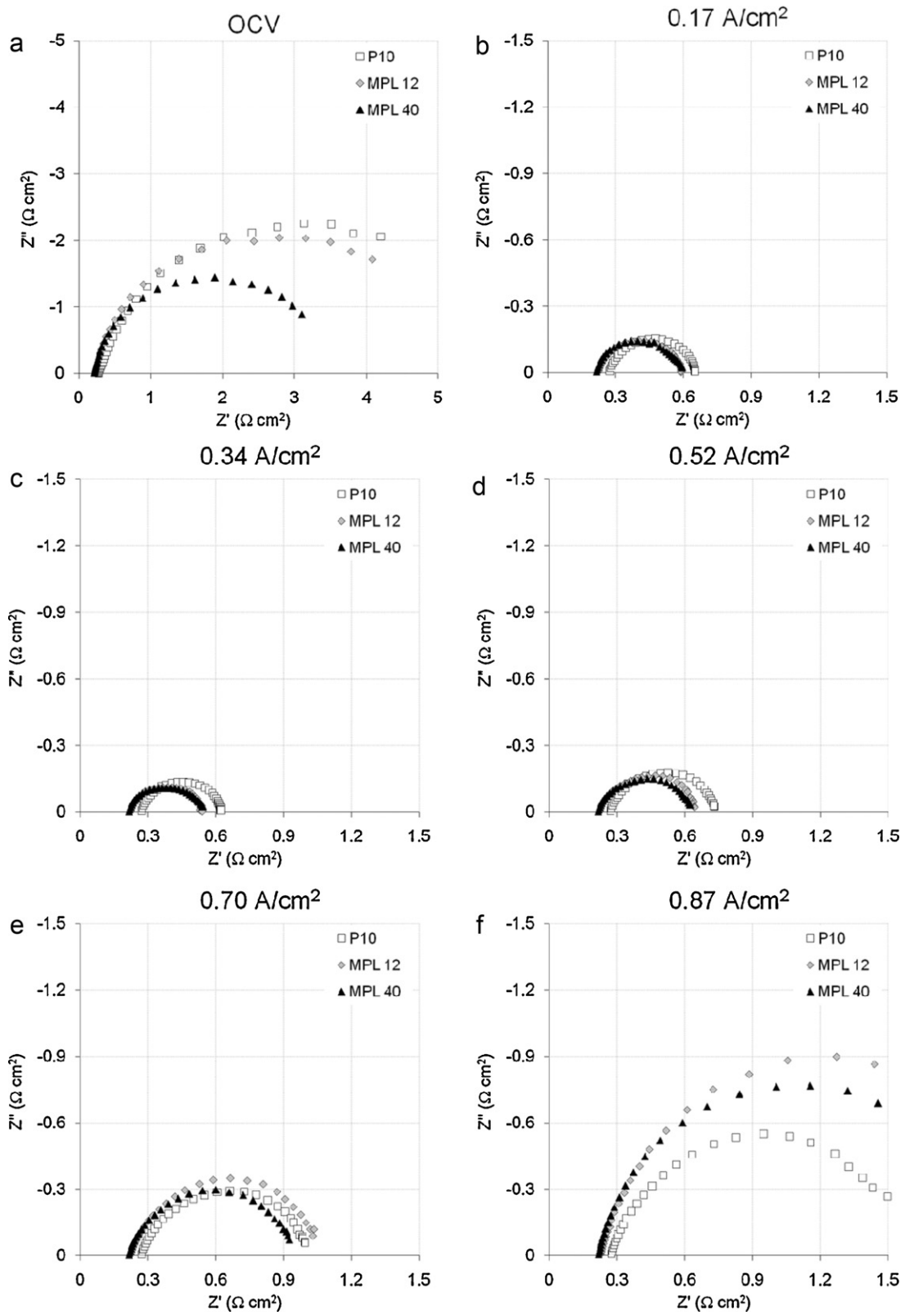

Fig. 6. Impedance spectra of the unit cell operating at 80 °C with a CR of 50% at increasing CD: (a) OCV, (b) 0.17 A cm^{-2}, (c) 0.34 A cm^{-2}, (d) 0.52 A cm^{-2}, (e) 0.70 A cm^{-2}, and (f) 0.87 A cm^{-2}.

much more one single arc slightly depressed; accordingly, it was impossible to fit them with the complete equivalent circuit that was used in all the other cases; so it was reduced to only one R/C parallel element, and the analysis of the relaxation frequencies confirmed the lack of the diffusive contribution.

When operating at 60 °C (Fig. 3), the overall cell resistance (right intercept of the spectra with the real axis) decreases abruptly passing from the OCV to 0.17 A cm^{-2}, then stays almost constant up to 0.34 A cm^{-2} and finally starts again increasing up to the highest CD values. Only in the case of MPL40 there is a slight decrease in the

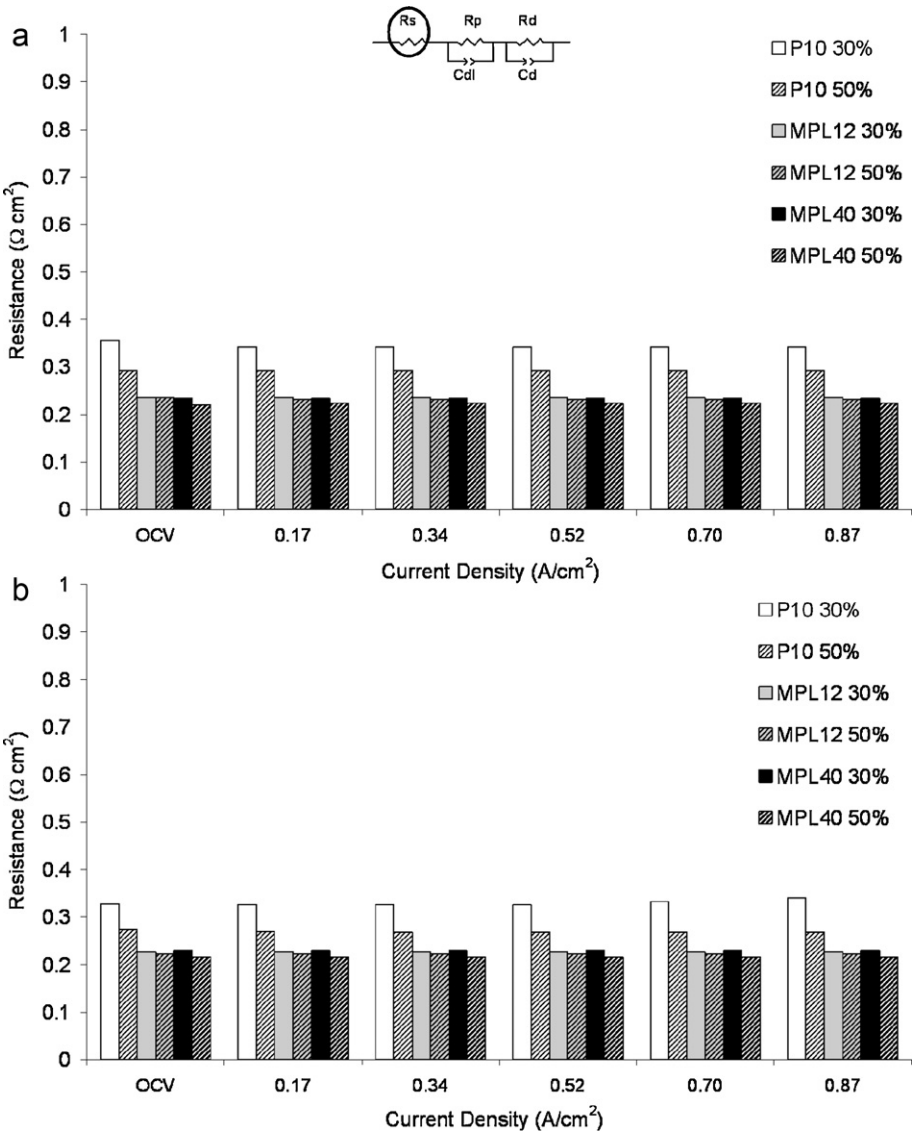

Fig. 7. Fitting results from the impedance spectra; ohmic resistance (Rs) (a) at 60 °C and (b) at 80 °C at increasing CD: OCV, 0.17 A cm^{-2}, 0.34 A cm^{-2}, 0.52 A cm^{-2}, 0.70 A cm^{-2}, and 0.87 A cm^{-2}.

overall cell resistance in the interval 0.17–0.34 A cm^{-2} (Fig. 3b and c). The resistance of the P10 assembly is greater than that of both MPL12 and MPL40 up to 0.52 A cm^{-2}, and then MPL12 outweighs the other two assemblies. It is remarkable that P10 assembly resistance changes very slightly at high CD, i.e. from 0.70 to 0.87 A cm^{-2}, while those incorporating the MPL increase more sensibly and at the highest CD, i.e. 0.87 A cm^{-2}, MPL12 outweighs P10.

The general trend is quite similar at the higher operating temperature (Fig. 4), i.e. 80 °C, but with some differences: overall cell resistance of all three assemblies decreases from 0.17 to 0.34 A cm^{-2}. Comparing the cell response at the two operating temperatures, at 80 °C total resistances are consistently lower at each CD, in accordance with the polarization and power curves (Fig. 2) showing a superior cell performance.

In general, the trend of impedance spectra at increasing CD is analogous when the compression ratio is raised to 50% (Figs. 5 and 6), with the overall cell resistance constantly higher than at CR = 30%, in accordance with cell performances that are worse (Fig. 2). Besides temperature has the same beneficial effect, namely it reduces the cell resistance at every CD.

All spectra were fitted with the equivalent circuit discussed in Section 2.4 and the results are reported in Figs. 7–9.

Ohmic resistance (Rs), which arises from bulk resistance of the membrane and GDL and from contact resistances (i.e. GDL – bipolar plate and GDL – catalyst layer), is markedly higher in P10 than in MPL12 or MPL40 (Fig. 7), although the GDLs coated with the MPL are even thicker than P10 (Table 2). The intrinsic surface anisotropy and poor surface smoothness typical of a cloth probably do not guarantee an optimal contact between GDL and catalyst layer/bipolar plate; in turn, this adversely affects contact resistances and then ohmic resistance.

Moreover, ohmic resistance of P10 assembly is sensibly improved by increasing the compression ratio, while the effect is practically inappreciable in the case of the other two GDLs. In addition to this piece of evidence, for all three assemblies Rs does not vary upon increasing CD, pointing out that the membrane is probably highly humidified at all CDs. Increasing the cell operating temperature from 60 to 80 °C (Fig. 7a and b) has no effect on Rs. In view of all these considerations it seems reasonable to attribute the difference between the three GDLs mainly to contact resistances. Moreover, MPL12 and MPL40 assemblies have the same Rs values notwithstanding the different amounts of hydrophobic agent; this fact which should affect the trough-plane resistance of GDLs is probably

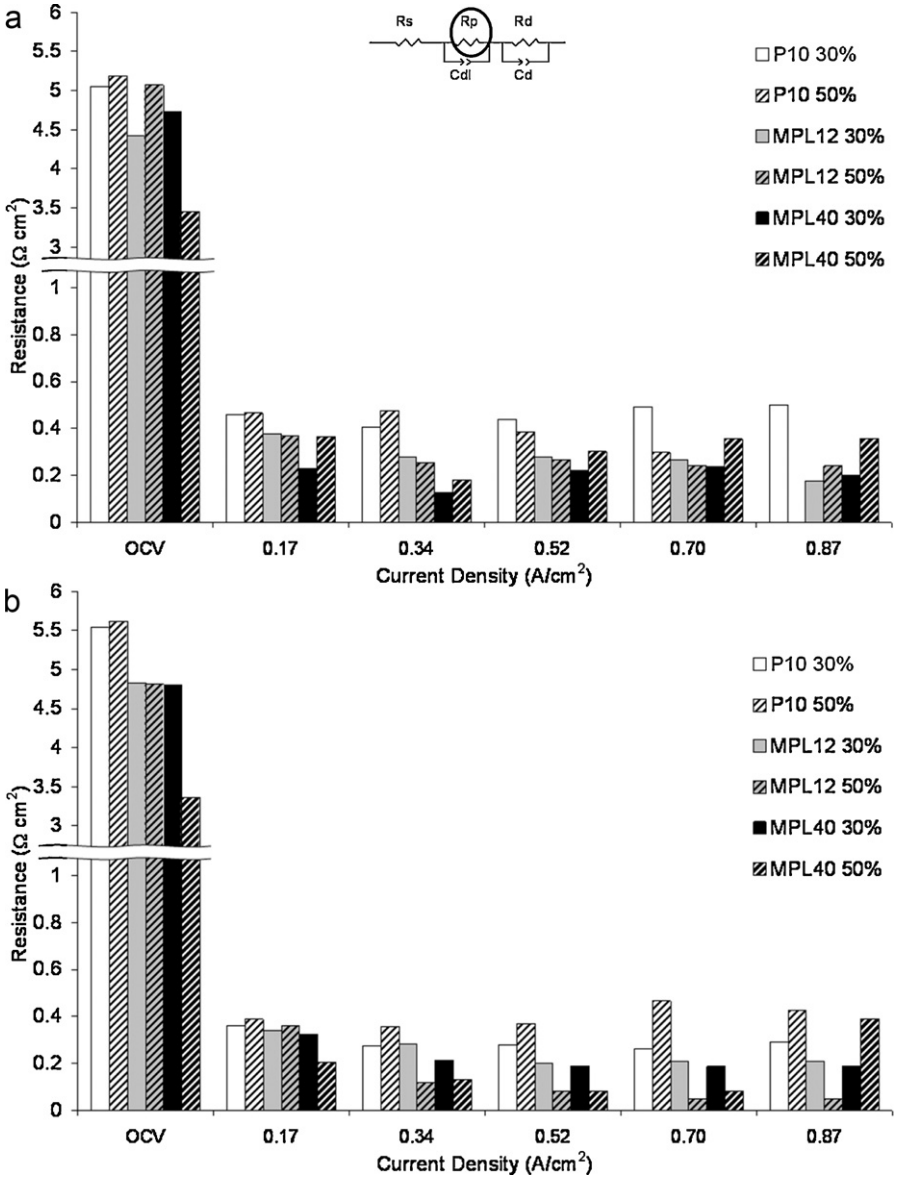

Fig. 8. Fitting results from the impedance spectra; polarization resistance (Rp) (a) at 60 °C and (b) at 80 °C at increasing CD: OCV, 0.17 A cm^{-2}, 0.34 A cm^{-2}, 0.52 A cm^{-2}, 0.70 A cm^{-2}, and 0.87 A cm^{-2}.

compensated by the different thicknesses of the MPL coatings (Fig. 1).

On average, polarization resistance (Rp) is very high at OCV, greatly decreases in the low CD region (0.17–0.34 A cm^{-2}) and then stays quite constant up to 0.87 A cm^{-2} (Fig. 8) for each assembly. This is consistent with the fact that at low CD polarization losses are mainly due to the oxygen reduction reaction (ORR) whose kinetics is much slower than that of hydrogen oxidation and then they tend to decrease when the current is raised [17].

In general, the increase in cell operating temperature reduces Rp, while the influence of the compression ratio is more variable. At 60 °C CR tends to worsen Rp in the medium to high CD range for MPL40, while does not have any appreciable influence on MPL12 except at 0.87 A cm^{-2}. At 80 °C CR increase affects positively both MPL12 and MPL40, but negatively P10; a worsening effect on MPL40 is registered only at 0.87 A cm^{-2}.

Although electron transfer processes, which are responsible of polarization losses, are certainly favoured by good contacts between GDL and CL, and increasing CR help reduce contact resistances, there are also other factors that impinge on Rp. First, lack of reactants, especially at high CD when their need is at maximum, slows down the kinetics of electrode reactions, and the compression certainly reduces the MPL pore volume which in turn makes more difficult for the reactants to reach the CL. Temperature increase can only partially alleviate this drawback.

Diffusion resistance (Rd), arising from mass transfer losses, becomes appreciable only at high CD (Fig. 9), when reactant consumption is larger and risk of flooding very likely if water management fails. In this event, water flooding clogs the pores, especially the micropores, drastically reducing gas feeding. Indeed, cell compression brings about an increase in Rd at high CD and the increase is more marked in the GDLs with MPL. This was not surprising because the carbon cloth is macroporous and the porosity reduction caused by compression is certainly less dramatic than for the MPL. In any case, the failure of P10 assembly at high CD has to be ascribed mainly to mass transfer and polarization losses which increase with CR (Figs. 8 and 9) and not to ohmic resistance which decreases (Fig. 7).

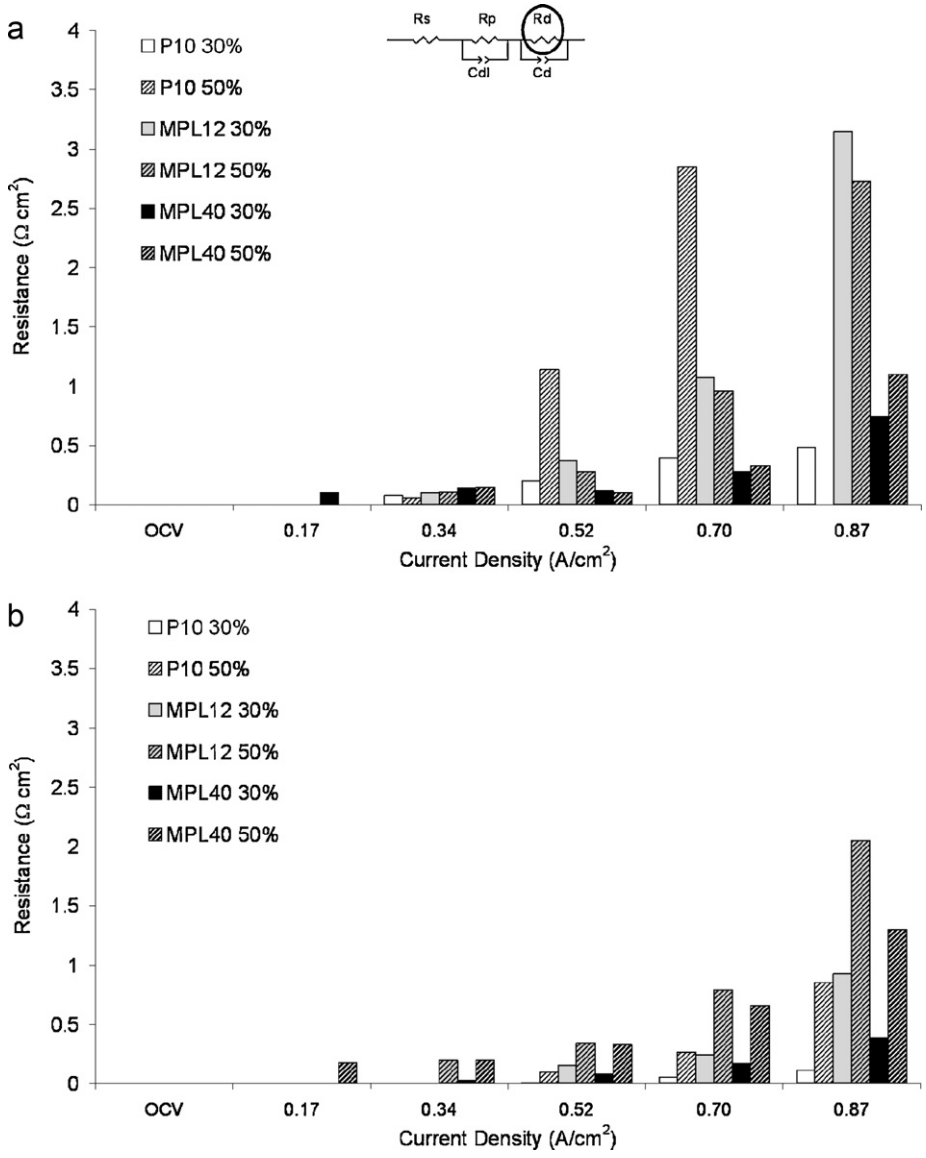

Fig. 9. Fitting results from the impedance spectra; diffusion resistance (Rd) (a) at 60 °C and (b) at 80 °C at increasing CD: OCV, 0.17 A cm^{-2}, 0.34 A cm^{-2}, 0.52 A cm^{-2}, 0.70 A cm^{-2}, and 0.87 A cm^{-2}.

In the literature there is a general consensus about the fact that compression increases mass transport resistance and decreases contact resistance [13–16], so that there could be an optimal compression ratio for the cell performances due to a careful balance between the two, as was recently found [26].

The better performances of MPL40 over MPL12 assembly (Fig. 2) were finally explained by comparing Rd values which result markedly lower for MPL40 (Fig. 9).

4. Conclusions

In the present work three carbon cloth-based GDLs, one without MPL and two with MPL, were tested at two different clamping pressures to assess the influence of GDL compression, i.e. 30 and 50%, on FC performances. The effect of operating temperature and MPL hydrophobicity were also taken into account. Impedance spectroscopy was carried out to highlight which factors influenced more the FC performances.

In general, it was observed that:

(1) Ohmic resistance Rs and mass transfer resistance Rd were more sensibly affected by the increase in CR suggesting that two contrasting phenomena occur when the GDL is compressed: contact resistance improvement between cell components and worsening of gas feeding;
(2) The increase of GDL compression from 30% to 50% had an adverse effect on FC performance only at high CD, even in the case of P10 assembly where the ohmic resistance decreased upon increasing the CR; this confirms the idea that a good performance comes from a careful balance between contact and mass transfer resistance;
(3) The use of a MPL coated onto the carbon cloth had an evident beneficial effect on FC performances, mainly due to a reduction in contact resistance as revealed by the ohmic resistance;
(4) The increase of operating temperature may be of help anyway, as it brings about a general decrease in every resistance contribution;

(5) The hydrophobicity of the MPL, which had a good influence on FC performances, turned out to come from a decrease in mass transfer resistance at high CD when more water has to be removed from the CL.

Acknowledgements

The Authors thank Fondazione Cariplo for financial support (Project 2008-2372: "Advanced Materials for Gas Diffusion Electrodes (GDE) in Polymer Electrolytes Membranes Fuel Cells (PEMFCs): Superhydrophobic Textiles and Nanocarbon-based Inks").

References

[1] O. Erdinc, M. Uzunoglu, Renew. Sust. Energy Rev. 14 (2010) 2874–2884.
[2] Yu.M. Volfkovich, V.E. Sosenkin, V.S. Bagotsky, J. Power Sources 195 (2010) 5429–5441.
[3] R. Andersona, L. Zhanga, Y. Dinga, M. Blancoa, X. Bia, D.P. Wilkinson, J. Power Sources 195 (2010) 4531–4553.
[4] M. Ji, Z. Wei, Energies 2 (2009) 1057–1106.
[5] H. Li, Y. Tang, Z. Wang, Z. Shi, S. Wu, D. Songa, J. Zhang, K. Fatih, J. Zhang, H. Wang, Z. Liu, R. Abouatallah, A. Mazza, J. Power Sources 178 (2008) 103–117.
[6] P. Gallo Stampino, G. Dotelli, L. Omati, P. Fracas, D. Brivio, P. Grassini, Smart Text. 60 (2009) 128–133.
[7] J.T. Gostick, M.A. Ioannidis, M.W. Fowler, M.D. Pritzker, Electrochem. Commun. 11 (2009) 576.
[8] J.H. Kang, K.-J. Lee, J.H. Nam, C.-J. Kim, H.S. Park, S. Lee, I. Kwang, J. Power Sources 195 (2010) 2608–2612.
[9] M. Rebai, M. Prat, J. Power Sources 192 (2009) 534.
[10] J.H. Nam, K.-J. Lee, G.-S. Hwang, C.-J. Kim, M. Kaviany, Int. J. Heat Mass Transf. 52 (2009) 2779–2791.
[11] J.H. Kang, K.-J. Lee, S.H. Yu, J.H. Nam*, C.-J. Kim, Int. J. Hydrogen Energy 35 (2010) 4264–4269.
[12] J.T. Gostick, M.A. Ioannidis, M.W. Fowler, M.D. Pritzker, J. Power Sources 194 (2009) 433–444.
[13] X.Q. Xing, K.W. Lum, H.J. Poh, Y.L. Wu, J. Power Sources 195 (2010) 62–68.
[14] J.-H. Lin, W.-H. Chem, Y.-J. Su, T.-H. Ko, Fuel 87 (2008) 2420–2424.
[15] J. Ge, A. Higier, H. Liu, J. Power Sources 159 (2006) 922–927.
[16] W-k. Lee, C.-H. Ho, J.W. Van Zee, M. Murthy, J. Power Sources 84 (1999) 45–51.
[17] N. Wagner, J. Appl. Electrochem. 32 (2002) 859–863.
[18] X. Yuan, H. Wang, J.C. Sun, J. Zhang, Int. J. Hydrogen Energy 32 (2007) 4365–4380.
[19] J. Wu, X.Z. Yuan, H. Wang, M. Blanco, J.J. Martin, J. Zhang, Int. J. Hydrogen Energy 33 (2008) 1735–1746.
[20] S. Asghari, A. Mokmeli, M. Samavati, Int. J. Hydrogen Energy 35 (2010) 9283–9290.
[21] P. Gallo Stampino, L. Omati, C. Cristiani, G. Dotelli, Fuel Cells 10 (2010) 270–277.
[22] G. Dotelli, L. Omati, P. Gallo Stampino, D. Brivio, P. Grassini, ECS Trans. 33 (2010) 1115–1122.
[23] P. Gallo Stampino, C. Cristiani, G. Dotelli, L. Omati, L. Zampori, R. Pelosato, M. Guilizzoni, Catal. Today 147S (2009) S30–S35.
[24] R.P Ramasamy, E.C. Kumbur, M.M. Mench, W. Liu, D. Moore, M. Murthy, Int. J. Hydrogen Energy 33 (2008) 3351.
[25] F.E. Hizir, S.O. Ural, E.C. Kumbur, M.M. Mench, J. Power Sources 195 (2010) 3463–3471.
[26] S.-D. Yim, B.-J. Kim, Y.-J. Sohn, Y.-G. Yoon, G.-G. Park, W.-Y. Lee, C.-S. Kim, Y.C. Kim, Curr. Appl. Phys. 10 (2010) S59–S61.